

INFULLENCE OF ADDING MCMBS INTO C/C COMPOSITES ON THEIR MICROSTRUCTURE AND MECHANICAL PROPERTIES AND DURING GRAPHITIZATION

Hsien-Lin Hu¹, Chih-Jong Chang¹, Jen-Dong Hwang¹ and Tse-Hao Ko²

¹*Materials and Chemical Research Laboratory, Industrial Technology Research Institute, Hsinchu Taiwan, R. O.C.*

²*Department of material sciences and Engineering, Feng Chia University, Taichung, Taiwan, R. O. C.*

Abstract

Carbon/Carbon composites were prepared from oxidative PAN fiber felts, resol- type phenolic resin and MCMB derived from coal tar. In this study, the effect on microstructure, flexural strength, flexural moduli, electric conductivity and thermal conductivity of carbon/carbon composites with MBMC content ranging from 0 to 30 wt.% was examined during pyrolysis. Results showed carbon/carbon composite with addition of 10 ~30 wt.% MCMB having higher density, greater size (L_c), and higher preferred orientation than for carbon/carbon composites without MCMB during heat-treatment. These composites also exhibited an improvement in flexural strength from 19.7% to 30.3%. Flexural moduli of these composites added with MCMB is increased by 15.1% to 31.3% as compared to that of the zero wt.% MCMB added composites. These composites also showed improved electric conductivity from 15.1% to 43.7% and thermal conductivity from 12 % to 31.3%.

1.Introduction

Carbon fiber/carbon matrix composites are regarded as the materials with the best structures for potential application in a high-temperature environment, due to their light weight, high thermal shock resistance, low thermal expansion and relatively high strength/stiffness at high temperatures 1-3. Combining their excellent thermal shock, ablation resistance and unique mechanical properties at high temperature causes C/C composites to be used in industry for manufacturing items such as brakes, nozzles, et al. They can also be used at intermediate temperatures (200-1000°C) in applications in which reinforced polymers cannot be used, such as connecting rods and pistons. In earlier research, expensive high-modulus carbon fibers and techniques have been used to produce these composites. However, a high demand for industrial applications has resulted in development of alternative fabrication routes with lower costs, along with controlled mechanical and thermal properties. In aerospace applications, 2D-C/C composites have been made from woven carbon fabrics as reinforcements.

2.Experiments

2.1 Raw materials

The C/C composites were reinforced with oxidative PAN fiber felts (Toho Rayon Co., Ltd., Japan). Resol-type phenol-formaldehyde resin (Chang Chum Petrochemical Industry Co., Taiwan) was used as matrix precursor; mesophase spheres (China Steel Chemical Co. Taiwan) were extracted from coal tar.

2.2 Fabrication

Resol-type-phenol-formaldehyde resin was dissolved in methanol. Then 10 wt% and 30 wt % mesophase spheres were added to resin and mixed with phenolic resin. Figure 1 presents fabrication procedures. First, oxidative PAN-based fiber felts were embedded into resins mixed homogenously with 0, 10 and 30 wt% mesophase spheres for 30 minutes in a vacuum. Second, impregnated samples were cured at 80°C for 2 hours, hot-pressed at 30 kg/cm² and 120°C for 30 minutes and 160°C for 10 minutes Then polymer composites were cut to appropriate size. Finally, the cut samples were stabilized at 230°C and pyrolyzed at a heating rate of 0.5°C/min up to 600, 1000, 1300 and 1500°C for carbonization; these composites were heat-treated at a rate of 10°C/ minute up to 1800 and 2500°C for graphitization.

2.3 Measurements

A Rigaku X-ray diffractometer with Cu K α radiation source was used to determine d space and stacking size (L_c , stacking height of layer planes) of composites, a Scherrer equation ⁴ to calculate stacking size from the width of a (002) reflection, B:

$$L_c = \frac{k\lambda}{B \cos\theta} \quad (1)$$

where $\lambda=0.154$ nm; k the apparatus constant (=1.0) and B half the width of the carbon- carbon composites. The width increases as the stacking size (L_c) declines. The flexural strength of composites was determined by the three-point bending method under ASTM D790.

3.Results and Discussions

3.1 X-ray diffraction

Figure 1 displays X-ray patterns for a composite following pyrolysis at various temperatures. Figure 4 indicates these patterns showed a broad peak at $2\theta \approx 22.4^\circ$ for composite R0, one at $2\theta \approx 23.19^\circ$ for M10 and one at $2\theta \approx 25.36^\circ$ for M30. Regarding R0, a broad and weak peak at $2\theta \approx 22.4^\circ$ was associated with transformation of noncarbon materials in the phenolic resin into glass carbon. Composites M10 and M30 include two peaks: one associated with phenolic resin, the other with mesophase spheres. At 600-1500°C, the intensities of peaks corresponding to (002) and (10 ℓ) reflection for carbon increased with temperature of heat treatment, and patterns revealed structure of Sample R0 as amorphous. Adding mesophase spheres caused the intensity of peaks of the (002) and (10 ℓ) planes to rise faster with temperature. Heat treatment at 1800°C precipitated conversion of non-graphite carbon in a graphite-like carbon structure. Unlike patterns of composites M10 and M30, those of composite R0 are somewhat amorphous, in that phenolic resin is hard carbon. Furthermore, continuously raising temperature of heat treatment to 2500°C causes intensities of peaks at (002) and (10 ℓ) reflections to become stronger, and the half-width of the peak of the (002) basal plane of the carbon to decline, as shown in Figure 1, due to graphitic planes' reorientation growing more extensive. Table 1 lists stacking sizes (L_c) of the (002) plane and interlayer spacing (d_{002}) of composites after pyrolysis at various temperatures. For all composites, the interlayer spacing clearly decreases while stacking size increases very slowly with the rise in temperature of heat treatment. Notably, adding mesophase spheres effectively raised L_c at 2500°C, yielding a stacking size of 3.1 nm for composite R0, 10.99 nm for composite M10 and of 18.20 nm for composite M30.

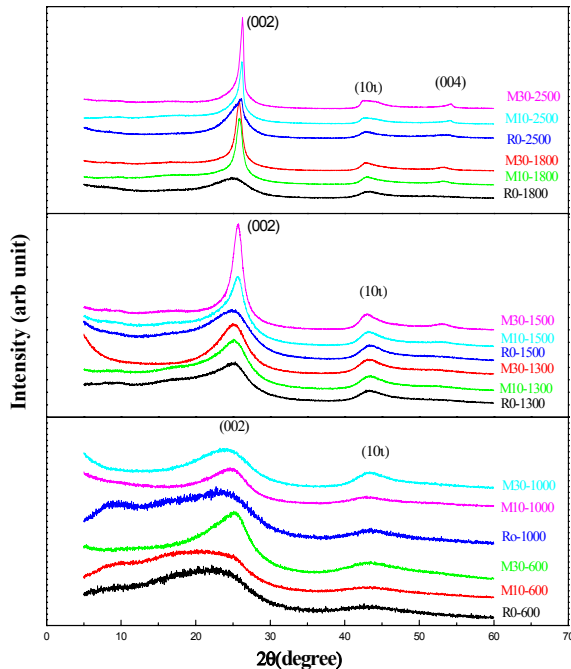


Table 1. X-ray Diffraction Results of the R0, M10 and M30 Composites Treated at various Temperature

	Carbonization and Graphitization Temperature(°C)					
	600	1000	1300	1500	1800	2500
Composite R0						
2θ (degree)	22.438	24.403	25.353	25.362	25.334	25.381
Interlayer Space d (nm)	0.397	0.362	0.358	0.354	0.352	0.350
Stacking Size L_c (nm)	0.861	1.363	1.438	1.674	2.259	3.104
Composite M10						
2θ (degree)	23.192	24.954	25.138	25.354	25.758	26.133
Interlayer Space d (nm)	0.373	0.359	0.354	0.348	0.353	0.341
Stacking Size L_c (nm)	0.878	1.398	2.214	2.633	6.787	10.992
Composite M30						
2θ (degree)	25.361	25.456	25.153	25.956	25.964	26.151
Interlayer Space d (nm)	0.364	0.354	0.348	0.342	0.337	0.341
Stacking Size L_c (nm)	0.959	1.543	2.353	3.073	9.129	18.200

Figure 1. The change in X-ray Diffraction pattern of composites at different heat treatment temperature

3.2 Polarized optical microscopy

Polarized light is often used to observe interference color generated by orientation of graphitic lamellae at the surface.^{5,6} Figure 2 traces such polarized-light optical micrographs of these carbon/carbon composites at various temperatures, along with a cross-polarized light micrograph of composites heat-treated at various temperatures. For composite R0, bonding between the fibers and matrix was strong because many functional groups were present on the surface of the oxidative PAN fiber, as depicted in Figure 2(a)-(c). The core of fibers is represented by light blue and bright blue colors at 600, 1500 and 2500°C, indicating the fibers have an anisotropic texture and heat-treatment enhances preferred orientation of the carbon layer in fibers. The matrix has an isotropic texture, as indicated by purple color in the matrix. The matrix derived from the phenolic resin is non-graphitizable carbon with a glass-like isotropic texture. Following graphitization at 2500°C, preferential orientation of the matrix is parallel to the fiber axis around the fibers, as revealed by micrographs in Figure 2 (c). In the area around the fibers, the matrix was graphitized and exhibited a preferred orientation of the carbon layers with an isotropic texture, since stress-orientation arose from strong bonding between the fiber and matrix, forming a region oriented parallel to the fiber surface at the interface in fibers. In the case of composites M10 and M30, as in Figures 2 (d)-(i), the MCMBs clearly exhibited light blue and bright blue colors at 600, 1500 and 2500°C, respectively, revealing that MCMBs and fibers have anisotropic texture. On the other hand, at 2500°C, the small areas around microcracks surrounding MCMBs in composites M10 and M30 showed light blue colors. It also indicated an anisotropic texture: thermal stress caused by differing thermal shrinkage rates of phenolic resin and MCMBs engendered an anisotropic texture, thus helping to improve flexural strength and moduli of composites M10 and M30 above 1800°C. The micrographs reveal the microcracks surrounding MCMBs were formed by the difference between shrinkage rates of the phenolic resin and MCMBs.

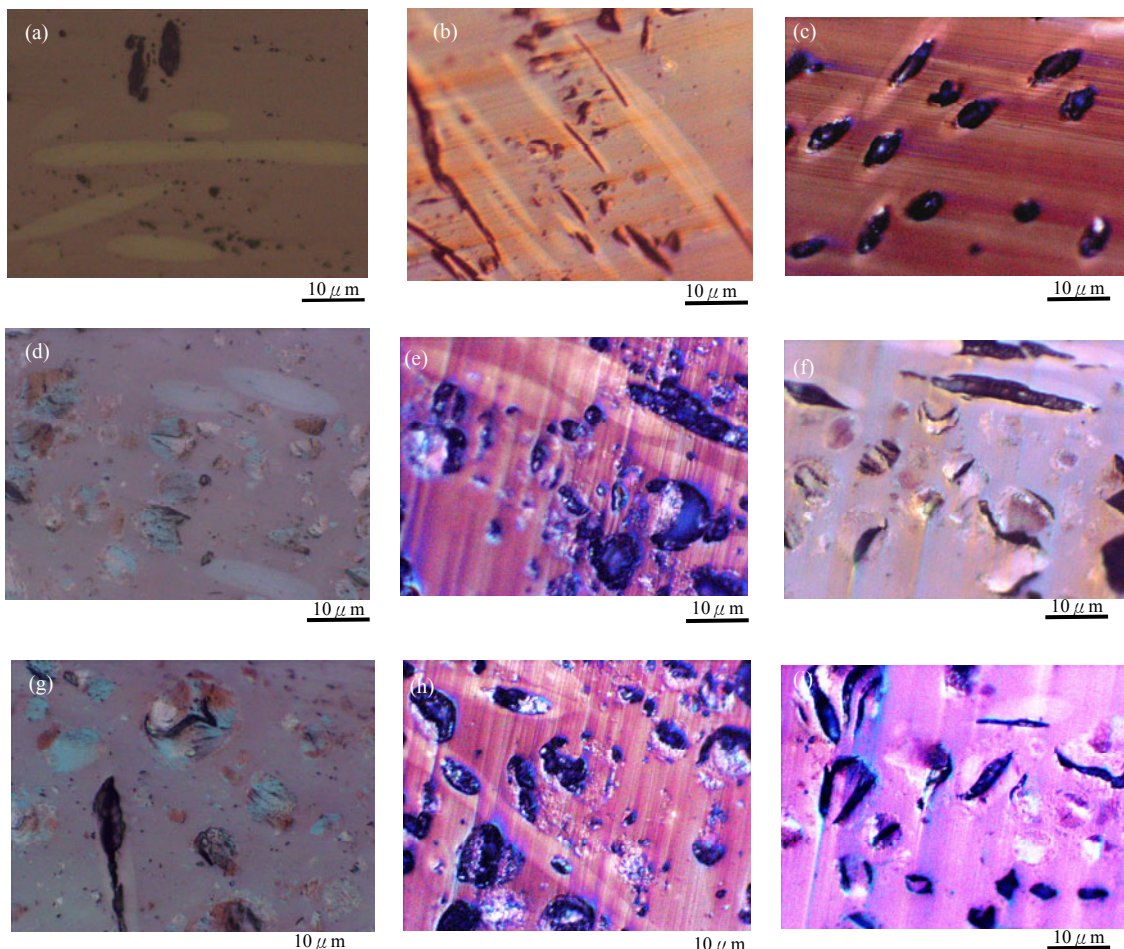


Figure 2. Polarized-light optical micrographs of carbon/ carbon composites at different heat treatment temperature.

3.5 Mechanical properties

Figure 3 (a) shows the model to measure mechanical properties. Figure 8 plots the variations in flexural strength and modulus of composites R0, M10 and M30 versus temperature at 600-2500°C. Figure 3 reveals how initial flexural strength and modulus of all composites at 600°C is low because of condensation of the polymer structures in the resin⁷ and crosslinks in the oxidative PAN fiber felts.⁸ Additionally, abrupt increases in flexural strength for all composites are observed at 600-1000°C. In this phase, carbon basal planes formed from the ladder polymer, increasing the preferred orientation, density and modulus.⁹ Yet glass carbon structures were transformed into isotropic carbon structures in the matrix resin. These reactions increase the flexural strength and modulus of composites, such that they led to flexural strength and moduli of composites M10 and M30 lower than those of R0. From 1000 to 1500°C, flexural strength and moduli of all composites decreased quickly by virtue of an increase in microcracks and formation of closed pores. Above 1800°C, the flexural strength of all composites increases slightly because conversion of non-graphite carbon in graphite-like carbon structure begins. At 2500°C, flexural strength of composite R0 is 15.4 MPa, M10 18.4 MPa and M30 22.4 MPa. Continuous decline in flexural moduli of composite R0 is observed above 1800°C while flexural moduli of composites M10 and M30 increase slightly. At 2500°C, flexural modulus of composite R0 is 1.65GPa, M10 1.9 GPa and M30 2.4 GPa.

In this work, the flexural strength and moduli of composites M10 and M30 are lower than those of R0 below 1800°C. However, the flexural strength and moduli of composites M10 and M30 exceed those of R0 above 1800°C. Below 1800°C, pores and cracks that surround MCMBs (Figures 2(b)) in composites M10 and M30 become centers of stress concentration and propagation, making the flexural strength and modulus of these composites lower than those of R0.

Above 1800°C, these small areas surrounding MCMBs and microcracks in phenolic matrixes showed anisotropic texture (Figures 2(h)-(i)). Such anisotropic texture (graphitizable carbon) emanated from both interface bonding and interface stress between MCMBs and phenolic resin. The interface stress was caused by different shrinkage rate between MCMBs and phenolic resin during graphitization. MCMBs were extracted from coal-tar in air at 400-600°C, so MCMBs also had some functional groups. These functional groups in both phenolic resin and MCMBs took chemical reaction to form strong interface bonding during the curing process as well as interface bonding between oxidative fibers and resin. Ko et al.²⁻⁹ reported that interface bonding between oxidative fibers and phenolic resin caused small anisotropy texture around fibers after graphitization. Ko et al.¹⁰ also described small anisotropy textures around fibers enhancing flexural strength and moduli. In present work, these small anisotropic textures surrounding MCMBs and microcracks were regarded as a factor to increase of flexural moduli of composites M10 and M30, compared with composite R0. For the flexural strength, these interface stress between MCMBs and resin in composites M10 and M30 above 1800°C also played an important role. Interface stress would block or change direction of microcrack propagation and thereby cause increase of flexural strength in composites M10 and M30, compared with composite R0.

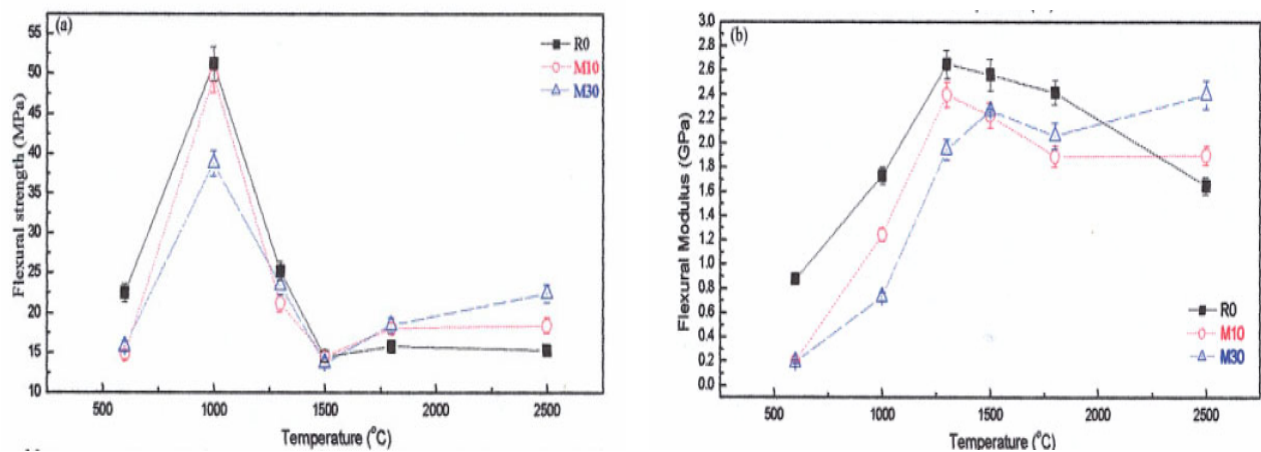


Figure 3. The change in the flexural strength and modulus of composites R0, M10 and M30 with heat treatment temperature in the range 600 to 2500°C.

4. Conclusion

The influence of adding MCMBs to microstructure and Mechanical properties of carbon/carbon composites prepared by pyrolyzing oxidative PAN fiber felt/phenolic resin was gauged via heat treatment at 600-2500°C. X-ray diffraction (L_C) and polarized-light optical microscopy established differences between microstructures of the resin and mesophase during co-graphitization. They reveal that MCMBs and oxidative PAN fibers exhibit anisotropic textures, whereas phenolic matrix has an isotropic texture following graphitization. This trait shows how phenolic resin and MCMBs are non-graphitizable and graphitizable carbon, respectively. Though the flexural strength and flexural moduli of composites with MCMBs added are lower than those without MCMBs below 1500°C, flexural strength and flexural moduli of composites with MCMBs exceed those without MCMBs above 1800°C. This fact may be associated with the strengthening of preferred orientation of a carbon layer plane with MCMBs added to composites.

Reference

1. Hüttener, W. Carbon Fibers Filament and Composites; Kluwer Academic: Boston, 1990; p 275.
2. Manocha, L. M. Sadhana Academy Proceeding in Engineering Sciences 2003, 28, 349.
3. Savage G. Carbon-carbon composites; Chapman and Hill: London, 1993; Chap 9.
4. Cullity, B. D. Element of X-ray diffraction; Wesley: New York, 1978; p. 99.
5. Eswards, I. A. S; Marsh, H. Introduction to Carbon Science; Butterworths: London, 1989; p 19.
6. Comford, C. R., Forrest, A. B., Kelly, T., Marsh, H.; Walk, P. L., Radovi, L. R. Chemistry and Physics of Carbon; Marcel Dekker: New York, 1984, 19; p 211.
7. Hishiyama, Y., Inagaki M., Kimura, S., Yamada, S. Carbon 1974, 12, 249.
8. Donnet, J. B., Wang, T. K., Peng, J. C. Carbon Fibers; Marcel Dekker: New York; 1998; p 26
9. Watt, W., Johnson, W. Nature 1975, 257, 210.
10. Ko, T. K., Kuo, W. S., Chang, Y. H. Composite: Part A 2003, 34, p393